Study of rotor asymmetry by finite element model of the induction machine

LEBAROUD Abdesselam[1] , CLERC Guy[2]

[1] Université 20 Août 1955, Skikda, et le laboratoire LEC, email: lebaroud@yahoo.fr
[2] Université de Lyon, Lyon, F-69622, France ; université Lyon 1, Lyon, F-69622, France ; CNRS, UMR5005, Laboratoire AMPERE, Villeurbanne, F-69622, France

Abstract

This paper presents the analysis of rotor asymmetry, caused by broken bars, and their effects on the stator current of an induction machine under unbalanced supply voltage.The simulation of the induction machine is based on the finite element method. Experimental tests corroborate with the simulation results.

1. Introduction

The main effect of the broken bars is the amplitude modulation of the stator current. It is characterized by the upper and lower sidebands; Filippetti [1] has explained how the interaction of the $(1-2ks)f_s$ harmonic of the motor current with the fundamental air-gap flux produces speed ripple at $2sf_s$ and gives rise to additional motor current harmonics at frequencies $(1+2ks)f_s$. Perovic [2] showed that when faults of both broken bars and stator turns short-circuit appear at the same time, the sideband components are $(1\pm 2ks)f_s$ and $-(1\pm 2\mathrm{ks})\mathrm{f_s}$ they appear respectively around the fundamental (f_s) and of the negative sequence current $(-f_s)$. Subhasis [3] demonstrated that broken bars sidebands also appear around 5th and 7th time harmonics. Researches on rotor dissymmetry are focused only on the formula (1), on the other hand the latter describes only the visible part of the fault. In order to show all the broken rotor bar frequencies in the motor current for both healthy and fault machine a more precise model is needed. The analytical models dedicated to the diagnosis and which are developed in the literature [4],[5],[6] are often penalized by simplified assumptions, in particularly the distribution of the magnetic flux density in the air-gap. The important information is likely to be omitted partially or completely if one considers only the fundamental of the magnetic flux density. However, a more precise model of the machine is necessary for an accurate analysis of the machine behavior in both healthy and faulty cases. A detailed analysis of broken rotor bar requires a precise model. They represent the electrical behaviour of the equivalent induction machine. The analytical models, also, do not take into account the electric or magnetic phenomena such as induced currents, magnetic saturation and the effect of complex geometry. Therefore these assumptions lead to the omission of relevant information on the machine condition. For a more precise modelling of the induction machine, it is necessary to consider its electromagnetic behaviour. The numerical resolution of Maxwell's equations governing the machine operation, and the reduction of simplifications introduced in the previous models, lead to a model closer to the real machine. The two-dimensional modelling of the induction machine reduces greatly the computation time and memory space used. The magnetic losses due to coils head are taken into account. In this paper, we use a model based on a magnetodynamic and transient magnetic formulation of the induction motor using the "Flux 2d" software. The simulation and the experimental verification allow an accurate analysis of the effects of broken bars with the consideration of the stator currents non ideal.

2. Finite element model of induction motor

The study of electromagnetic systems behaviour depends on their operating modes. Indeed, several formulations are possible such as electrostatics, electrodynamics, the magnetostatic, the magnetodynamic, etc.. Since the induction motor has a dynamic that we cannot neglect in the study, our choice fall on a study magneto-evolving, and this allows to following the temporal and transient behaviour of the machine.

The software used in this study is Flux2D @ Cedrat [7]. This latter allows achieving magnetic circuit scheme in two dimensions. Our choice is oriented towards the plane which is perpendicular to the rotation axis of the machine and which develops the electromagnetic field.

The magneto-evolutionary model is represented by the following equation:

$$\sigma_e \frac{d\vec{A}}{dt} + rot\vec{}\left(\frac{1}{\mu rot\vec{}\left(\vec{A}\right)}\right) = J + rot\vec{}\left(\vec{H}\right) \qquad (1)$$

A : magnetic vector potential (Wb/m)
J : current density uniform (A/m)
μ : magnetic permeability (H/m)
H : magnetic field (A/m)
σ_e : electrical conductivity ($1/\Omega.m$)
T : Time (seconds)

3. Electrical circuit of rotor

Electrical circuit of rotor (fig.1) contains three elements: Massive conductor, Resistance of ring and leakage inductance. Resistance additional was added within circuit in order to simulate the broken bar. The calculation of leakage inductance takes into account the permeance of stator slots because it is considered that the surface of slot in the magnetic circuit is completely filled with copper. Against the permeance of isthmus and head coil are considered in the magnetic representation.

For the rotor (Figure.1), we have the following scheme

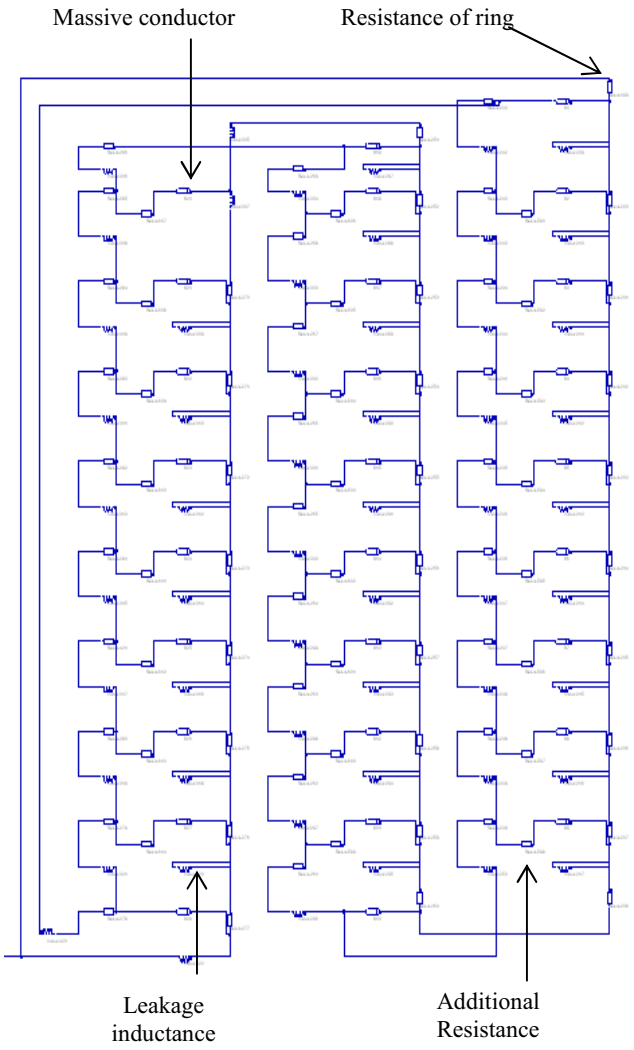

Fig. 1. Electric circuit of stator

Solid conductors represent rotor bars and they are related to the magnetic circuit. These conductors are connected by resistors and inductors represent respectively the resistance of rings portions (2) and Leakage inductance of rings portions and the bars permeance (3). Their calculations are developed in Annex 1 and are of the form:

$$R_{ann} = \rho_{Al} \frac{l_{an}}{N_R S_{an}} \tag{2}$$

$$L_{fr} = P_{fer} + \frac{P_{fann}}{2\sin\left(\frac{p\pi}{N_R}\right)^2} \tag{3}$$

The assignment of elements of stator and rotor electrical circuits to magnetic circuit are performs in an interactive manner through the software flux 2d.

4. Simulation

4.1. Healthy machine

The components of electrical circuit are assigned to the magnetic circuit (Figure.2 a,b). Magnetization of the machine to the initial state is made by a magneto-dynamic resolution. The latter is independent of time. When the machine has been magnetized, we launched the magneto- evolutionary resolution. Thus, the speed of rotation is imposed constant equal to 1440 rpm and simulation of stator current begins by a transitional regime (Figure.2). Figure 2a shows the distribution of equiflux lines in the magnetic circuit, with the presence of symmetry in relation to inter-polar axis. The lines of flux between the stator and rotor are slightly deflected in the direction of rotation of the rotor. The distribution of induction in Figure 2a is also quasi-symmetric.

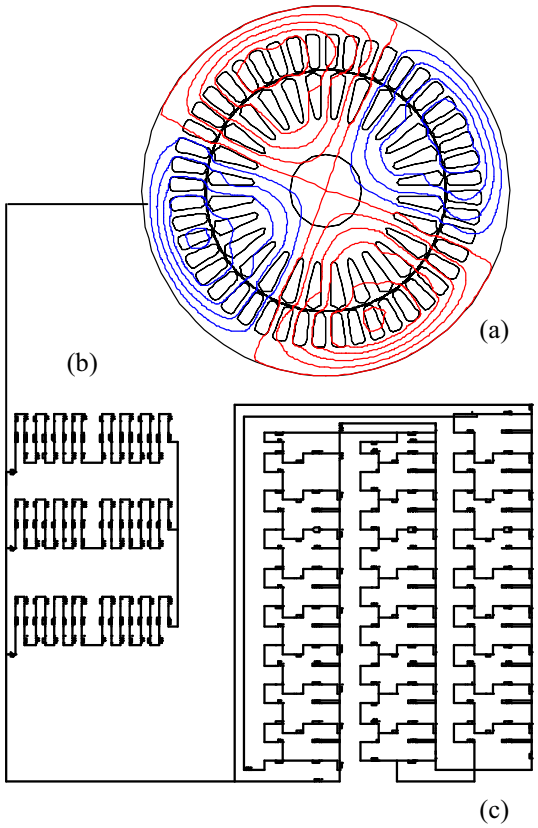

Fig.2. Induction machine model
(a) machine Geometry
(b) stator windings
(c) rotor Model

4.2. Broken rotor bars

To illustrate the broken bars in the rotor circuit, we have assigned a value of almost infinite to the resistance which is in series with the bar, in the electrical system of the rotor. The area representing the broken bar in the magnetic circuit is filled by a non-magnetic material. As a result, electric current is no longer circulating in the broken bar, but this one has a material effect on the distribution of field lines. It is well known that the broken bars induced electromotive force (emf) in the stator windings at frequencies around of stator current fundamental. In this study, we want to study the effect, due to broken of bars, on the stator current with a not ideal supply. The simulation

model of the machine in the healthy case and faulty case is shown in Figures 3 and 4. The model was subjected to an unbalance in supply voltage. Two broken bars induced of sidebands in the spectrum of stator current. These bands appear around the fundamental (*f*) and its inverse symmetrical component (*-f*). These sidebands are shown in Figures 3and 4 by part (a). However, there are also other side bands, shown in Figures 3 and 4 in frames (b), at frequencies 22, 26 Hz and 70 Hz, 74 Hz, but this time correspond to the expression of Deleroi.

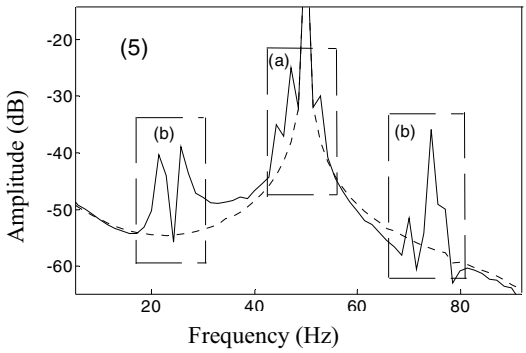

Fig.3. Spectrum of stator current vector of four bar broken (solid), healthy (dashed))

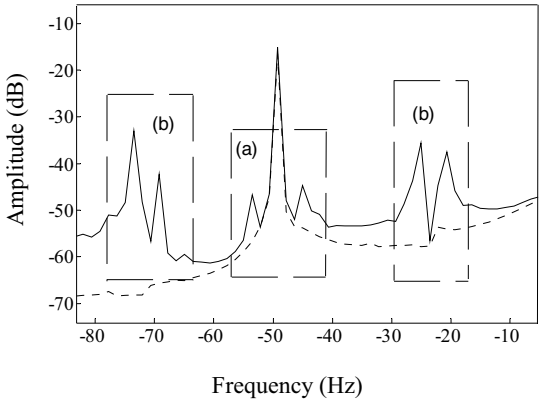

Fig.4. Spectrum of inverse sequence component of four bar broken (solid), healthy (dashed))

5. Experimental Results

The experimental bench consists of a three-phase asynchronous motor squirrel cage Leroy Somer LS 132S, IP 55, Class F, T° C standard = 40 ° C. The motor is loaded by a brake powder. Its maximum torque (100 Nm) is reached at rated speed. This brake is designed in order to dissipate a maximum power of 5 kW. The figure 5 below shows the bench motor.

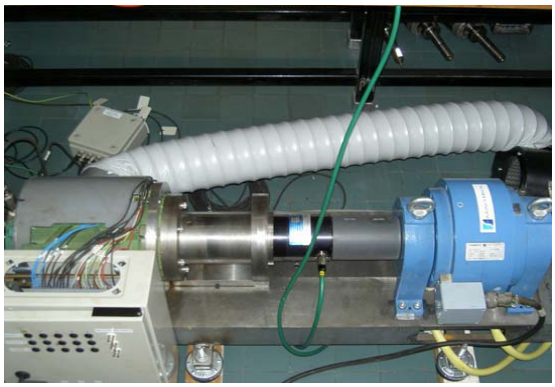

Fig.5. Test bench of induction motor

Fig.6. Broken bars (1,2,3)

For the rotor fault, the bar has been broken by drilling bar of cage squirrel (Fig.6). The 5% of unbalance supply, is obtained with a variable autotransformers placed on a phase of the network (Fig.5). An acquisition of current signals was carried out on a test bench, The sampling rate is 10 KHz. The number of samples per signal rises to N=10000 samples. Test is then performed on current signals collected at the 25% and 70% load levels.

Figure 7 shows the spectrum of the vector space of stator currents. We notice that the broken bars faults induced sidebands around the following frequencies: the fundamental 50 Hz (Figure 7), the inverse sequence component -50 Hz (Figure 8), harmonics -250 Hz (Figure 9) and harmonics 350 Hz (Figure 10). Therefore these results are validated by those of the simulation.

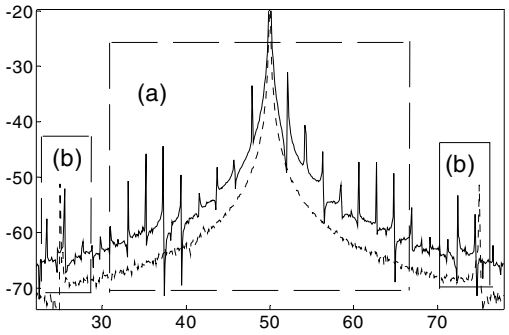

Fig.7. Spectrum of vector space of the stator current, three broken bars (solid), healthy (dashed)

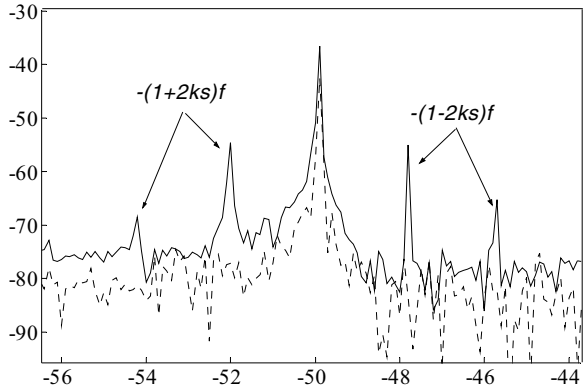

Fig.8. Zoom on the vector space of the stator current in spectrum domain, three broken bars (solid), healthy (dashed)

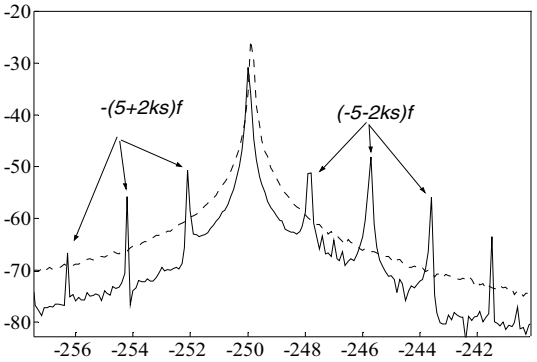

Fig.9. Zoom on the vector space of the stator current in spectrum domain, three broken bars (solid), healthy (dashed)

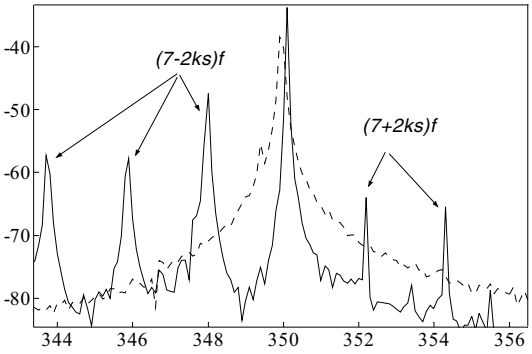

Fig.10. Zoom on the vector space of the stator current in spectrum domain, three broken bars (solid), healthy (dashed)

6. Conclusions

Simulation of the induction machine by finite element method yielded good information on the electrical behaviour of the machine in both healthy case and faulty case. The simulation of broken bars has allowed highlighting all the sidebands related to faults. Early detection is possible from components located around the fundamental frequency (*f*), around the inverse sequence component *(- f)* and around the odd frequency.

7. References

[1] F. Filipetti, G. Franceschini, C. Tassoni, P. Vas "AI techniques in induction machine diagnosis including the speed ripple effect", California, vol 1, IAS, , pp 655-662, 1996.

[2] D.K. Perovic, M. Arkan, P. Unsworth "Induction motor fault detection by space vector angular fluctuation", IEEE IAS, Rome, Italy, Vol 1, pp 388-394, 2000.

[3] N.Subhasis, B. RajMohan, H.Toliyat, G. Alexander "Study of three phase induction motors with incipient rotor cage faults under different supply conditions", IEEE-IAS annual meeting conference, Phoenix, AZ, Oct. 3-9, pp.197-204, 1999.

[4] E. Ritchie, X. Deng, T. Jokinen. " Dynamic model of 3-phase squirrel cage induction motors with rotor faults ", ICEM 94, B6(2), pp.694-698, 1994.

[5] P.Vas, F. Filippetti, G. Franceschini, C. Tassoni, " Transient modelling oriented to diagnostics of induction machines with rotor asymmetries ", ICEM, pp.62-67,1994.

[6] A. Bentounsi, A. Nicolas "On line diagnosis of defaults on squirrel cage motors using FEM", IEEE Transactions on magnetics, vol. 34, no 5, Sept.1998.

[7] FLUX2D, CAD package for electromagnetic and thermal analysis using finite elements FLUX2D, Version 7.40, Induction Machine Tutorial, 1999.